ACADEMIC PRESS

Available online at www.sciencedirect.com

SCIENCE DIRECT®

DEVELOPMENTAL BIOLOGY

Developmental Biology 260 (2003) 31–45

www.elsevier.com/locate/ydbio

A role for programmed cell death during early neurogenesis in *Xenopus*

Weeteck Yeo and Jean Gautier*

Department of Genetics and Development, Columbia University, New York, NY 10032, USA

Received for publication 26 July 2002, revised 21 March 2003, accepted 3 April 2003

Abstract

In vertebrates, little is known on the role of programmed cell death (PCD) occurring within the population of dividing neural precursors and newly formed neuroblasts during early neural development. During primary neurogenesis, PCD takes place within the neuroectoderm of *Xenopus* embryos in a reproducible stereotypic pattern, suggesting a role for PCD during the early development of the CNS. We find that the spatio-temporal pattern of PCD is unaffected in embryos in which cell proliferation has been blocked and whose neuroecotoderm contains half the normal number of cells. This shows that PCD is not dependent on cell division. It further suggests that PCD does not solely function to regulate absolute cell numbers within the neuroectoderm. We demonstrate that PCD can be reproducibly inhibited in vivo during primary neurogenesis by the overexpression of human Bcl-2. Following PCD inhibition, normal neurogenesis is disrupted, as seen by the expansion of the expression domains of *XSox-2*, *XZicr-2*, *XNgnr-1*, *XMyT-1*, and *N-Tubulin*, *XNgnr-1* being the most affected. PCD inhibition, however, did not affect the outcome of lateral inhibition. We propose, then, that PCD regulates primary neurogenesis at the level of neuronal determination.

Keywords: *Xenopus*; Programmed cell death; Primary neurogenesis; Neuronal determination; Cell division; TUNEL; *Bcl-2*

Introduction

Programmed cell death (PCD) is an important process, taking place during the development of many tissues and organs in both vertebrates and invertebrates. Most PCD occurs via apoptosis, a well-characterized genetic program that exhibits specific morphological features, such as membrane blebbing, nuclear and cytoplasmic shrinkage, chromatin condensation, and DNA fragmentation (Kerr et al., 1972). DNA fragmentation enables the detection of apoptotic cells in situ via the TUNEL (Terminal deoxynucleotidyl transferase mediated dUTP Nick-End Labeling) technique (Gavrieli et al., 1992). The key effector components of apoptosis belong to a family of cysteine proteases named the caspases. Caspases are activated by proteolytic cleavage to form active oligomeric complexes, which then cleave selected intracellular proteins at specific aspartate residues (Nicholson and Thornberry, 1997). Thus, immunocytochemistry with antibodies directed against activated forms of caspases provides an alternative to TUNEL in the detection of apoptotic cells (Srinivasan et al., 1998).

Apoptosis is essential in the removal of structures such as the intersegmental musculature in insects, the tail in anurans during metamorphosis, or the interdigital mesenchyme in the development of the vertebrate limb (Jacobson et al., 1997). Many neurons die via apoptosis during the development of the peripheral nervous system, in the process of establishing proper synaptic organization and axonal pathways. PCD also participates in removing nonfunctional or even potentially harmful cells such as nonreactive or self-reactive B and T lymphocytes (Sanders and Wride, 1995).

The majority of studies on PCD in vertebrate development have focused either on postembryonic or on late embryonic development, while much less is known about the roles of PCD during the early phases of gastrulation and neurulation (Glucksmann, 1965; Jacobson et al., 1997). Recent studies using TUNEL have highlighted the occurrence of patterned PCD in the early stages of development in zebrafish, *Xenopus*, and chick (Cole and Ross, 2001; Hensey and Gautier, 1998; Hirata and Hall, 2000). In *Xe-*

* Corresponding author. Fax: +1-212-923-2090.
E-mail address: jg130@columbia.edu (J. Gautier).

0012-1606/03/$ – see front matter © 2003 Elsevier Science (USA). All rights reserved.
doi:10.1016/S0012-1606(03)00222-7

nopus, PCD is detected in a reproducible and dynamic pattern within the embryo from late gastrulation to late neurulation (Hensey and Gautier, 1998). Strikingly, PCD is detected exclusively within the presumptive neuroectoderm at the neural plate stage. As development proceeds, the pattern of PCD becomes more defined, confined within the anterior regions where the brain and sensory placodes will eventually form, and within the neural folds that will give rise to the spinal cord. At later stages, PCD remains localized to specific brain regions, developing sensory organs and the spinal cord. The reproducible and patterned cell death occurring within the developing neural tissues at early stages suggests a role for PCD in primary neurogenesis (Hensey and Gautier, 1998).

Primary neurogenesis occurs as a cascade of events taking place following neural induction of the dorsal ectoderm. Neural induction is mediated by the inhibition of BMPs by secreted factors from the organizer such as Chordin, Noggin, and Follistatin (Harland, 2000). Expression of early neural genes, such as *XSox-2*, occurs within the induced neuroectoderm, followed by the expression of *XNgnr-1*, a bHLH determination factor of neuronal fate, within three bilateral longitudinal domains within the neuroectoderm (Chitnis, 1999). Lateral inhibition within these domains restricts the number of neural cells specified to become neurons. Cells specified to become neurons express the Zn-finger neuronal specification factor *XMyT-1*, which enables them to escape lateral inhibition and eventually undergo neuronal differentiation, as seen by *N-Tubulin* expression (Sasai, 1998). Concomitant with this neurogenic cascade, cell proliferation is taking place within the neuroectoderm. Cell division occurs in a single wave, moving in a lateral to medial direction from stages 12 to 16 in *Xenopus* (Hartenstein, 1989).

Mice deficient in Casp-3, Casp-9, or Apaf-1 show defects in PCD and die before birth, suggesting that PCD is essential for proper embryonic development (Cecconi et al., 1998; Hakem et al., 1998; Kuida et al., 1996, 1998; Yoshida et al., 1998). The embryonic lethality could be due to the hyperplasia in the brain, a possible consequence of the lack of PCD in both undifferentiated neural precursors at the early stage, and differentiated neurons that do not establish the right synaptic connection in the later stages (Blaschke et al., 1996; de la Rosa and de Pablo, 2000; Kuan et al., 2000).

We have successfully prevented the occurrence of PCD in vivo during the early development of *Xenopus* embryos through the expression of human Bcl-2. We find that inhibition of PCD during early neurogenesis leads to the disruption of normal neurogenesis, resulting in the expansion in both neural and neuronal cell types. PCD is abrogated when neural cells are diverted from differentiation and maintained in an uncommitted state by the overexpression of constituitively active *X-Notch*^{ICD}, suggesting that PCD participates in primary neurogenesis at the level of neuronal determination. In addition, we show that the occurrence of PCD is independent of cell proliferation, establishing that its role is not limited to controlling the absolute cell number in the neuroecotderm or eliminating damaged, nonfunctional cells.

Materials and methods

Embryos

Albino *Xenopus laevis* embryos were obtained by in vitro fertilization and cultured using standard methods (Sive et al., 1994). Embryos were staged according to Nieuwkoop and Faber (1967).

Cell cycle inhibition

Embryos were dejellied in 2% cysteine, pH 7.8, grown to stage 10.5–11.0, and treated with proteinase-K (Roche) at 5 μg/ml for 5 min at room temperature to weaken the vitelline membrane. To block DNA synthesis, embryos were incubated in a solution of 20 mM hydroxyurea (Sigma) and 150 μM aphidicolin (Sigma) in 0.1× MMR (HUA), as described in Harris and Hartenstein (1991). Aphidicolin was diluted from a 10 mg/ml frozen stock in dimethyl sulfoxide (DMSO). Embryos were kept continuously in HUA at 14°C until fixation. To arrest cell cycle at M-phase, dejellied stage 11.0 embryos were incubated in a solution of 10 μM nocodazole (Sigma) in 0.1× MMR at 14°C until fixation. Nocodazole was diluted from a 10 mg/ml frozen stock in DMSO. All embryos were fixed in MEMFA (100 mM Mops, pH 7.4, 2 mM EGTA, 1 mM $MgSO_4$, 4% formaldehyde) and stored in methanol at −20°C.

RNAs and microinjection

Synthetic capped RNAs for microinjection were synthesized by in vitro transcription using mMessage mMachine kit (Ambion) and purified following manufacturer's instructions. *Bcl-2β* RNA was transcribed from pRC/CMV (Invitrogen, gift from Dr. T. Sato). *Bcl-2G145A* RNA was transcribed from pRC/CMV, subcloned from pGEM4Z (gift from Dr S. Korsmeyer; Yin et al., 1994). *GFP* RNA was transcribed from pCS2++ (gift from Dr A. Hemmati-Brivanlou), subcloned from pEGFP-N1 (Clontech). *X-Notch*^{ICD} and *X-Delta-1*^{STU} RNAs were transcribed from pCS2+ (gifts from Dr C. Kintner).

All RNAs were injected into either one or both blastomeres of two-cell stage embryos in 4% Ficoll, 1× MMR. The uninjected side was used as an internal control. For negative control, embryos were similarly injected with *GFP* RNA. RNAs were injected in a volume of 5 nl at concentrations of 20–300 pg/nl. Embryos were grown to neurulae stages and then fixed.

Animal caps assay and RT-PCR analysis

For animal cap experiments with RNA microinjection, animals caps were excised at stage 8.5–9.5 and cultured in 1× LCMR (66 mM NaCl, 1.33 mM KCl, 0.33 mM $CaCl_2$, 0.17 mM $MgCl_2$, 5 mM Hepes, pH 7.2) supplemented with 0.1% BSA and antibiotics (penicillin and streptomycin 100 μg/ml; gentamycin 50 μg/ml) until stage 19. RNA extraction was performed using RNA-Bee (Tel-Test, Inc.), followed by isopropanol precipitation. The following primer pairs used for RT-PCR analysis have been previously described: *EF1α* for 25 cycles (Agius et al., 2000), *XSox-2* for 25 cycles (Mizuseki et al., 1998), and *XBra* for 30 cycles (Agius et al., 2000). PCR products were analyzed on 2% agarose gel stained with Sybr-Gold (Molecular Probes) and visualized using the Fluoroimager (AP Biotech).

Whole-mount TUNEL staining

Whole-mount TUNEL protocol was performed as previously described (Hensey and Gautier, 1998). Briefly, embryos stored in methanol were rehydrated in PBS, permeablized in PBT (0.2% Tween 20 in PBS), washed in PBS, and incubated in 150 U/ml terminal deoxynucleotidyltransferase (GIBCO BRL) and 0.5 μM dioxigenin–dUTP (Roche). The reaction was stopped in PBS/1 mM EDTA, at 65°C, followed by washes in PBS. Detection and chromogenic reaction was carried out according to Harland (1991). The embryos were blocked in PBT + 20% goat serum, followed by incubation with anti-dioxigenin antibody coupled to alkaline phosphatase (Roche). Embryos were extensively washed in PBS and the staining was developed using nitro blue tetrazolium and 5-bromo-4-chloro-3-indolyl phosphate substrates. The reaction was visible within 30 min, and embryos were viewed following dehydration in methanol and mounted in benzyl benzoate/benzyl alcohol 2:1. Embryos were photographed on Zeiss Axiophot using Zeiss Axiovision 2.05 imaging system.

Whole-mount in situ hybridization and immunocytochemistry

Whole-mount in situ hybridization was performed as previously described (Chitnis et al., 1995) using digoxygenin-labeled antisense probes. Probes for *N-Tub* (Oschwald et al., 1991), *X-MyT1* (Bellefroid et al., 1996), *XZicr-2* (Brewster et al., 1998), *XMyoD* (Hopwood et al., 1989), *XNgnr-1* (Ma et al., 1996), *XSox-2* (Mizuseki et al., 1998), and *XDelta-1* (Chitnis et al., 1995) were prepared as described previously.

Immunocytochemistry was performed according to Harland (1991). Embryos were blocked in PBT + 20% goat serum for 1 h and then incubated at 4°C overnight, with anti-phosphorylated histone H3 antibody (1:1000, Upstate; Saka and Smith, 2001) for identification of mitotic cells, or with CM1 - anti P20 peptide of hCPP32 (1:2500, IDUN) for activated caspases detection. Embryos were extensively washed in PBS and the color reaction was developed using nitro blue tetrazolium and 5-bromo-4-chloro-3-indolyl phosphate substrates.

For double staining, the probe hybridization step of in situ hybridization was performed first followed by immunocytochemistry with anti-Bcl-2 antibody SC-100 (Santa Cruz) or anti-GFP antibody B-2 (Santa Cruz). Detection of antibodies was done using alkaline phosphatase conjugates with Fast Red (Roche) or 5-bromo-4-chloro-3-indolyl phosphate. The alkaline phosphatase was then inactivated by incubation in PBS containing 0.1 M EDTA at 65°C for 30 min. Unilaterally microinjected embryos were sorted based on which half was injected, indicated by immunocytochemistry. Some of the embryos stained with Fast Red were washed in 100% ethanol for 30 min to remove the red coloration before being subjected to the further chromogenic reactions. The digoxygenin-labeled probe was detected and visualized as described above, using nitro blue tetrazolium and 5-bromo-4-chloro-3 indolyl phosphate substrates.

All whole-mounts were photographed as described for TUNEL. Quantification of *N-Tub* expression was performed by measuring the area occupied by *N-Tub*-positive cells using SCION Image. The area of choice on the embryo was outlined on the image obtained from the Axiovision 2.05 system and measured.

Embedding and sectioning

Cleared embryos were washed in xylene, 1 × 5 min, 1 × 30 min. This was followed by a 30-min incubation in xylene:paraplast (1:1) at 55°C. Embryos were then transferred to paraplast and incubated for 3 × 30 min at 55°C. Embryos were positioned in molds, allowed to set overnight, and 10-μm sections were cut. Sections were dewaxed in Hemo-De (Fisher), mounted, counterstained with eosin, and photographed on a Zeiss Axioplan microscope using a Zeiss Axiovision 2.05 imaging system.

Western blot analysis

Embryos from stages 15 and 25 were collected and frozen in liquid nitrogen. Embryos were homogenized in XB buffer (100 mM KCl, 0.1 mM $CaCl_2$, 1 mM $MgCl_2$, 10 mM potassium Hepes, pH 7.7, 50 mM sucrose), and centrifuged at 13,000 rpm for 15 min at 4°C to remove the debris. The supernatant was then collected and used for Western blot analysis. Western blot analysis was performed using anti-Bcl2 antibody SC-100 (Santa Cruz) and PVDF membrane filters (Immobilon, Millipore). Signals were visualized using chemiluminescence (Amersham).

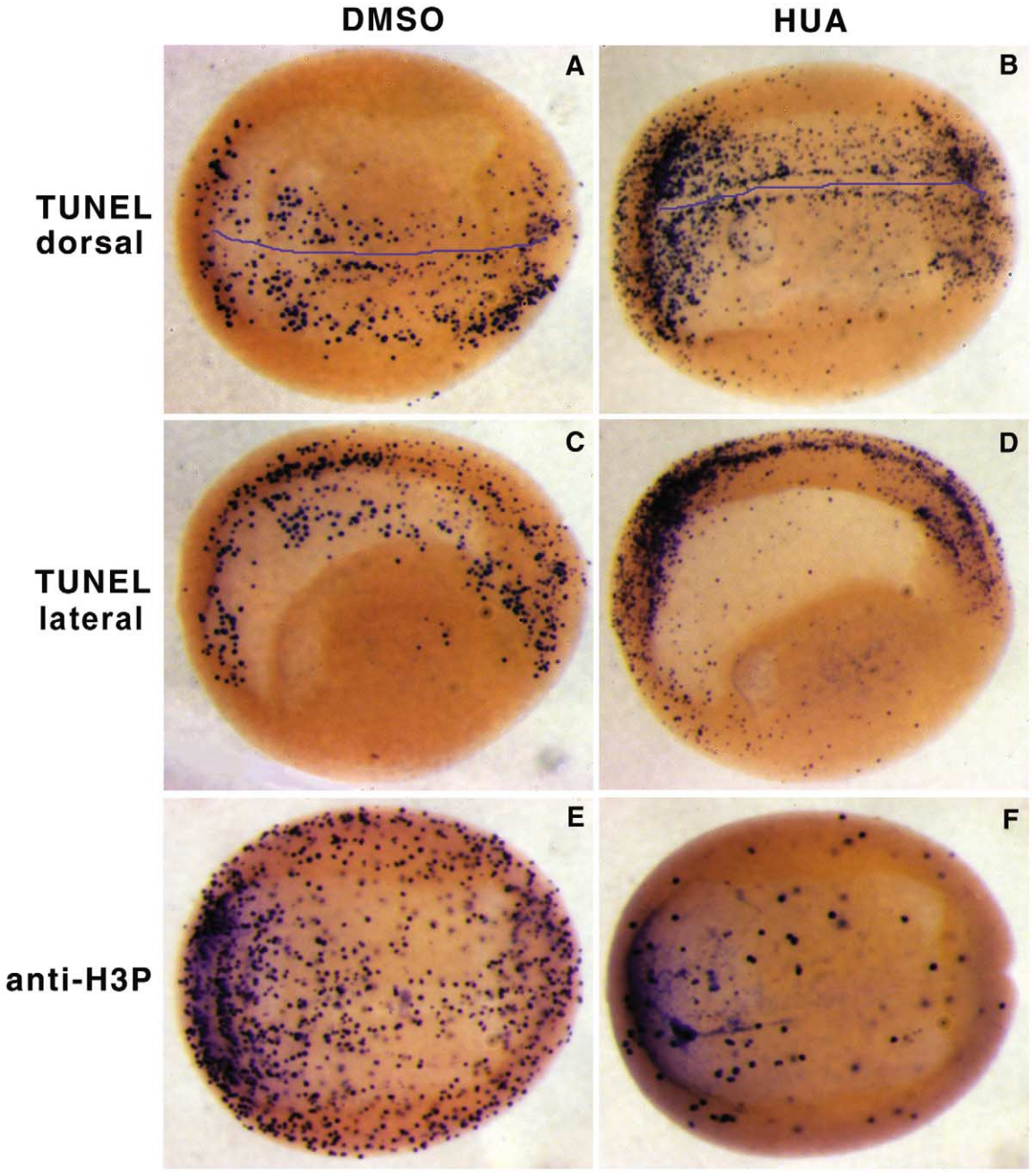

Fig. 1. Occurrence of PCD within the neuroectoderm is independent of cell proliferation. (A, B, E, F) Embryos shown in dorsal orientation; (C, D) embryos shown in lateral orientation; all embryos are cleared and shown with anterior to the left. (A, B) Blue lines indicate the position of the dorsal midline. (A–D) Whole-mount TUNEL staining of stage 15 embryos. (A, C) Control embryos incubated in DMSO; (B, D) embryos incubated in HUA (see Materials and methods). (E, F) Immunocytochemistry with anti-phosphorylated histone H3 in stage 15 embryos: (E) DMSO control; (F) HUA-treated embryo.

Results

Occurrence of PCD is independent of cell proliferation

To address the possible role of PCD during early neural development, we first determined whether PCD requires or is dependent upon the wave of cell division taking place within the neural plate. Indeed, the similarity between the spatio-temporal pattern of both proliferation and cell death suggests possible relationships and interaction between these physiological mechanisms in the regulation of the absolute number of cells within the developing neuroectoderm. Therefore, we investigated the spatio-temporal patterns of PCD in the absence of cell proliferation. Inhibition of cell proliferation was achieved by incubating the embryo in a mixture of HUA, which inhibits DNA synthesis in early S-phase of the cell cycle (Harris and Hartenstein, 1991). The effect of HUA on cell proliferation was monitored by

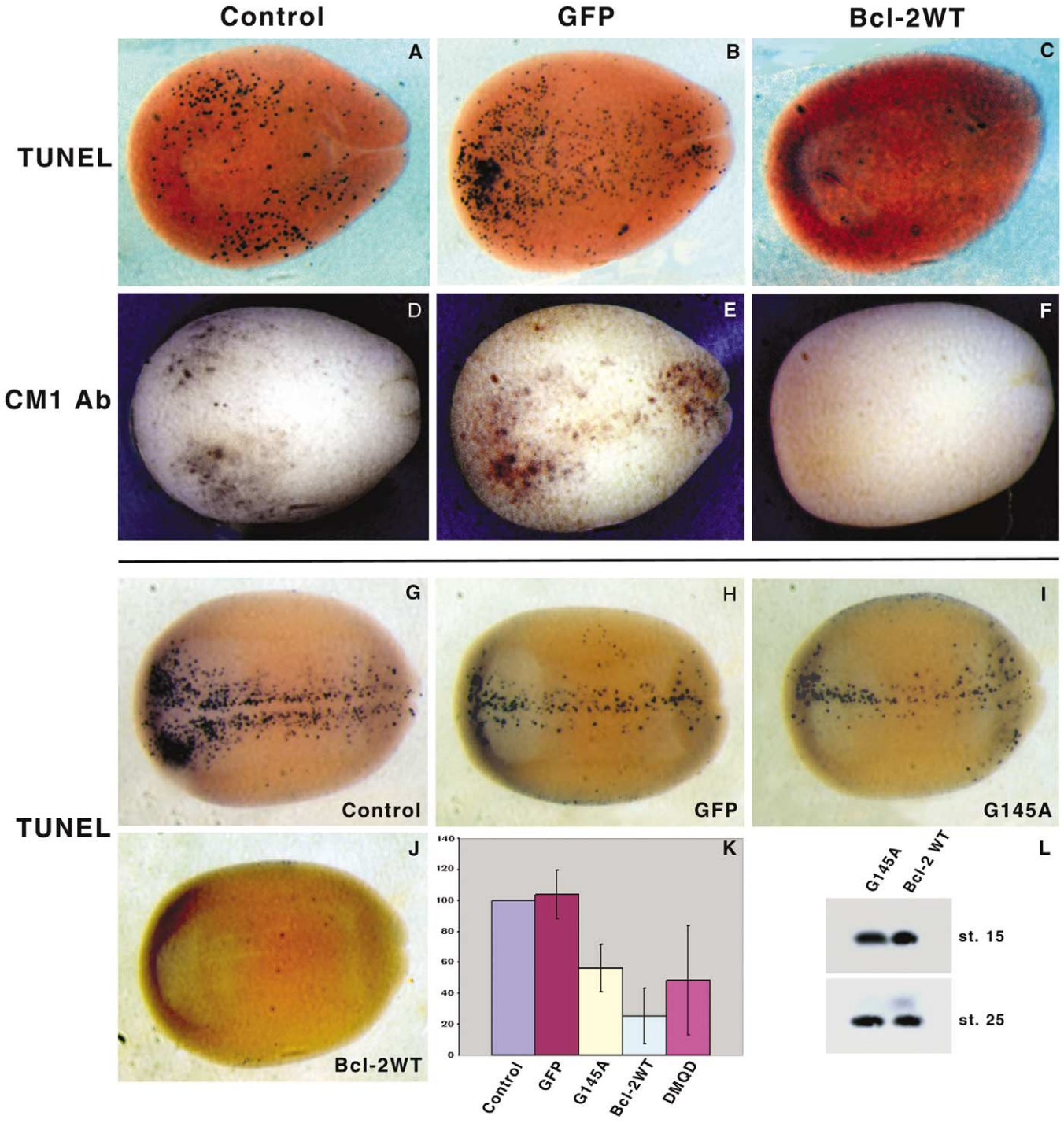

Fig. 2. Effect of Bcl-2 expression on programmed cell death in vivo. All injected embryos were injected at two-cell stage in both blastomeres. All embryos are shown in dorsal orientation with anterior to the left; TUNEL-stained embryos were cleared. (A–F) Effect of expression of human Bcl-2 on PCD during early neurogenesis. (A–C) Whole-mount TUNEL staining in embryos at stage 13; (A) uninjected control; (B) embryo injected with GFP mRNA (100 pg/nl); (C) embryo injected with *Bcl-2* mRNA (100 pg/nl). (D–F) Whole-mount immunocytochemistry with antibody against activated caspases, CM1, in embryos at stage 13: (D) uninjected control; (E) embryos injected with *GFP* mRNA (100 pg/nl); (F) embryo injected with *Bcl-2* mRNA (100pg/nl). (G–L) Levels of PCD inhibition by wild-type and mutant Bcl-2. (G–K) Whole-mount TUNEL staining in stage 16 embryos: (G) uninjected control; (H) embryo injected with *GFP* mRNA (20 pg/nl); (I) embryo injected with *G145A* mutant (20 pg/nl, see text); (J) embryos injected with wild-type *Bcl-2* mRNA (20 pg/nl). (K) Quantification of the inhibition on TUNEL done by the comparison of the percentage of TUNEL-positive embryos in each experimental batch with that from the uninjected control: Control: 100%; GFP: 104.0 ± 15.8%; G145A: 56.3 ± 8.6%; Bcl-2: 25.2 ± 4.6%; DMQD: 48.5 ± 17.2%. (L) Embryos injected with wild-type or *G145A Bcl-2* mRNAs were collected at stages 15 and 25, and processed for Western blotting using specific anti-Bcl-2 antibodies.

staining mitotic cells by immunocytochemistry with antibodies specific for phosphorylated histone H3, a specific marker of mitotic cells, thus establishing the efficacy of HUA treatment (Saka and Smith, 2001). Embryos incubated in HUA at stage 11 exhibited a dramatic decrease in the level of proliferation, seen by the number of mitotic cells, compared to that of the controls incubated in DMSO (Figs. 1E and F). TUNEL staining was still present, despite the dramatic decrease in cell proliferation in the HUA-treated embryos (Figs. 1A–D). The DMSO-treated controls displayed the typical TUNEL staining pattern: within the anterior neuroectoderm and posterior neural folds as expected for stage 15 (Figs. 1A and C; Hensey and Gautier, 1998). The HUA-treated embryos also displayed a similar pattern of staining, although at a higher level compared to the DMSO controls (Figs. 1A and B). Transverse sections of HUA-treated embryos showed that staining was still confined within the neuroectoderm, typical of PCD in the neuroectoderm (data not shown; Hensey and Gautier, 1998). We never observed any significant staining in tissues other than the neuroectoderm in stages 13 to 17, similar to that observed in untreated controls. Because variability exists in TUNEL staining (Hensey and Gautier, 1998), we quantitated the level of TUNEL staining by counting the embryos with more than 30 stained nuclei in the dorsal ecotoderm in both HUA-treated and DMSO-control batches; 83.0 $\pm$ 27.9% of HUA-treated embryos (454 embryos) exhibited positive staining, whereas only 34.3 $\pm$ 26.8% of DMSO embryos (425 embryos) exhibited positive staining. In addition, the density of staining was reproducibly stronger within the anterior neuroectoderm and posterior neural folds compared to that of the DMSO-treated control (Figs. 1C and D). In addition, TUNEL staining in HUA-treated embryos was greatly reduced when the embryos were microinjected with Bcl-2 mRNA at the two-cell stage (data not shown), demonstrating that the TUNEL staining observed in HUA-treated embryos was due to PCD. We conclude that PCD within the neuroectoderm during primary neurogenesis is not dependent on normal cell proliferation taking place within the neural plate. This indicates that the regulation of the absolute cell number of the neuroectoderm is not the primary role of PCD within the neuroectoderm.

Bcl-2 inhibits PCD in vivo

To assess the possible consequences of inhibiting PCD during the development of the neuroectoderm, we designed experimental conditions to inhibit PCD in vivo. We chose to express human Bcl-2 protein to prevent the occurrence of PCD (Fig. 2). We have previously demonstrated that human *Bcl-2* mRNA microinjection is very effective in inhibiting apoptosis triggered by irradiation in *Xenopus* eggs (Hensey and Gautier, 1997). We used two different assays to identify cells undergoing apoptosis: TUNEL staining, which identifies cells undergoing DNA fragmentation, and immunocyotchemistry, with an antibody (CM1) that specifically recognizes the activated forms of caspases (Gavrieli et al., 1992; Srinivasan et al., 1998). Importantly, both methods gave very similar staining patterns (Figs. 2A–F, data not shown). Specifically, CM1 staining was mostly confined within the dorsal region of early neurulae, similar to TUNEL staining (Figs. 1 A and D; Hensey and Gautier, 1998). This shows that the spatio-temporal pattern of caspase activation correlates with that of DNA fragmentation. Embryos injected with *Bcl-2* mRNA showed strong reduction in both TUNEL and CM1 staining (Figs. 2E and F), whereas those injected with *GFP* mRNA exhibited stainings confined to the neuroectoderm, similar to those observed for the noninjected controls (Figs. 2B and C). Hence, PCD during early development of the *Xenopus* embryo can be specifically inhibited in vivo by the expression of exogenous human anti-apoptotic Bcl-2. Furthermore, TUNEL staining is reduced significantly following microinjections with DMQD, a synthetic peptide inhibitor of the effector caspase Caspase-3, suggesting that Caspase-3 plays a significant role in bringing about PCD in the neuroectoderm (Fig. 2K; Talanian et al., 1997).

Studies in mammalian cells showed that the heterodimerization of Bcl-2 with pro-apoptotic protein Bax prevents Bax-dependent release of cytochrome c from the mitochondria and subsequent caspase activation (Chao and Korsmeyer, 1998; Desagher and Martinou, 2000). The G145A mutant form of Bcl-2 carries a missense mutation in its BH3 domain, impairing its interaction with Bax. As a result, the G145A mutant exhibits 30% of the wild-type anti-apoptotic activity (Yin et al., 1994). To determine if the exogenous-Bcl-2 protein inhibited apoptosis in a manner similar to that described in mammalian cells, we compared the effects of expressing wild-type Bcl-2 and the G145A mutant on PCD. Embryos injected with *GFP* mRNA did not exhibit any reduction in TUNEL staining, beyond that of the variability of the assay (Figs. 2G, H, and K). Embryos injected with the mutant G145A mRNA exhibited significantly higher TUNEL staining than that of embryos injected with wild-type *Bcl-2* mRNA (Figs. 2I, J, and K; *t*-test value <0.05), whereas the levels of expression for each protein were similar (Fig. 2L). However, the mutant still retained partial ability to inhibit PCD; embryos injected with the G145A mutant still displayed a significant reduction in overall TUNEL staining when compared to the unaffected uninjected and GFP controls (Fig. 2K, *t*-test value <0.05). This confirms that the reduction in TUNEL staining observed in *Bcl-2*-injected embryos is not due to a nonspecific effect of overexpressing the protein in these embryos. This further shows that reduction of TUNEL in *Bcl-2*-injected embryos is due to the documented anti-apoptotic activity described in mammalian cells. This strongly suggests that apoptosis within the neuroectoderm occurs via the mitochondrial pathway, regulated by interactions between proteins with functions homologous to that of Bcl-2 and Bax.

Taken together, these experiments establish that PCD can be reproducibly inhibited in vivo during early neuro-

genesis and that *Bcl-2* mRNA microinjection can be used as a reliable way to assess consequences of PCD inhibition on development.

PCD inhibition leads to an increase in neuronal cell numbers

We assessed the consequences of PCD inhibition on neural development following microinjection of Bcl-2 mRNA into one blastomere of two-cell stage embryos. Injected halves were visualized by immunocytochemistry using antibodies against GFP or Bcl-2. One example of GFP and *N-Tubulin* double-staining showing the injected half is presented in Fig. 3H (see Materials and methods). The red coloration indicating the injected half was then washed off after the injected embryos were sorted out based on which half had been injected, and before the examination of the expression pattern of any molecular marker. The consequence of PCD inhibition on the development of the neural plate was first monitored by following the expression pattern of *N-Tubulin,* an early marker of neuronal differentiation (Fig. 3A; Oschwald et al., 1991). Inhibition of PCD via Bcl-2 expression in one side of the embryo resulted in the lateral expansion of *N-Tub* expression domain on the injected side compared to that of the uninjected side (Figs. 3C–F; 30.5% in 400 *Bcl-2*-injected embryos). Control injections, using *GFP* mRNA, did not result in any significant difference in *N-Tub* expression pattern between the injected and uninjected sides compared to that observed in uninjected controls (Figs. 3A and B). Transverse sections of embryos exhibiting *N-Tub* expansion showed that the domain of *N-Tub*-positive cells corresponding to the position of prospective sensory neurons was expanded laterally (Fig. 3G). In addition, the medial domain corresponding to the motor neurons was expanded as well in slightly older embryos (data not shown).

To test that Bcl-2 did not directly modify ectodermal cell fate, animal cap explants from embryos overexpressing Bcl-2 were monitored for the expression of *XSox-2,* an early neural marker, and *Xbra,* a marker for axial mesoderm (Fig. 3I). *Bcl-2*-injected animal caps did not acquire mesodermal or neural identity as seen by the lack of *XSox-2* and *XBra* expression. However, *XSox-2* was induced in animal caps overexpressing neural inducer, Chordin. Furthermore, the effect of PCD inhibition on *N-Tub* expression, via Bcl-2 overexpression, did not vary within the range of *Bcl-2* mRNA microinjected (0.25–1.5 ng/embryo) that did not show any differential level of PCD inhibition (data not shown). This establishes that the expansion of *N-Tub* is specifically due to the inhibition of PCD, via the overexpression of Bcl-2, and suggests that PCD may regulate the development of primary neurons.

The nonneuronal domain between the lateral and the medial domains expressing *N-Tub* was also expanded at the posterior region of the embryo (Figs. 3C–F) and we followed the expression pattern of *XZicr-2,* which is expressed within this region (Fig. 3J; Brewster et al., 1998). *Bcl-2*-injected embryos showed an expansion in *XZicr-2* expression domain in the posterior region of the embryo, corresponding to the region between the medial and lateral neuronal domains (Fig. 3L; 24.3% in 58 *Bcl-2*-injected embryos), in agreement with the expanded *N-Tub*-negative region observed earlier. However, the expansion observed for *XZicr-2* was modest, compared to that observed for *N-Tub,* in terms of both the fraction of embryos displaying the expansion and the size of the expansion itself. GFP-injected control embryos did not exhibit such expansion (Fig. 3K). This confirms that PCD inhibition affects non-neuronal cells within the neuroectoderm as well, albeit at a less significant level than that observed for *N-Tub.*

We used two different methods to quantitate the effect of PCD inhibition on the expansion of the lateral *N-Tub* domain (Fig. 4). In the first method, we used *N-Tub*-positive cell count as the read-out (Fig. 4C). *N-Tub*-positive cells were counted for each half in the embryos injected with *Bcl-2*. The ratio of *N-Tub*-positive cells in the injected to uninjected was calculated (illustrated in Fig. 4A). The average ratio of *N-Tub*-positive cells in *Bcl-2*-injected half/uninjected half in the *Bcl-2*-injected batch was 1.43. This was significantly higher than the average ratio obtained for the entire GFP-injected batch, which was 0.94 (Fig. 4C, *t*-test value < 0.01). In the second method, we used the area of *N-Tub*-positive domain as the read-out (Fig. 4D). The area of the *N-Tub* domain on either side of the unilaterally injected embryos was drawn and measured using SCION Image software. The ratio between areas of *N-Tub* domain of the injected and uninjected sides was calculated (illustrated in Fig 4B). The average ratio of *Bcl-2*-injected was 1.47, whereas that of the *GFP*-injected batch was 0.97 (Fig. 4D, *t*-test value <0.01). Thus, when PCD was inhibited in one-half of the embryo, the number and the area of *N-Tub*-positive cells increased in that half. Taken together, these results confirm that PCD inhibition leads to increases in both the number of *N-Tub*-positive cells and the size of the neuroectoderm, supporting the qualitative observations (Fig. 3). Therefore, inhibition of PCD results in the disruption of normal neuronal development as seen by ectopic *N-Tub*-positive cells, accompanied by an increase in neural tissue.

Absence of PCD leads to expansion of neural tissue

N-Tub expression occurs as a consequence of the neurogenic cascade, which is initiated from the time of neural induction (Sasai, 1998). The abnormal expression pattern of *N-Tub* during PCD inhibition suggests that disruptions along this cascade have occurred as a result of PCD inhibition. As PCD occurs throughout the period during which neuronal differentiation takes place in the posterior neuroecotoderm, we first investigated the spatial expression of genes, specific to processes regulating neuronal differentiation within the three domains of primary neurogenesis

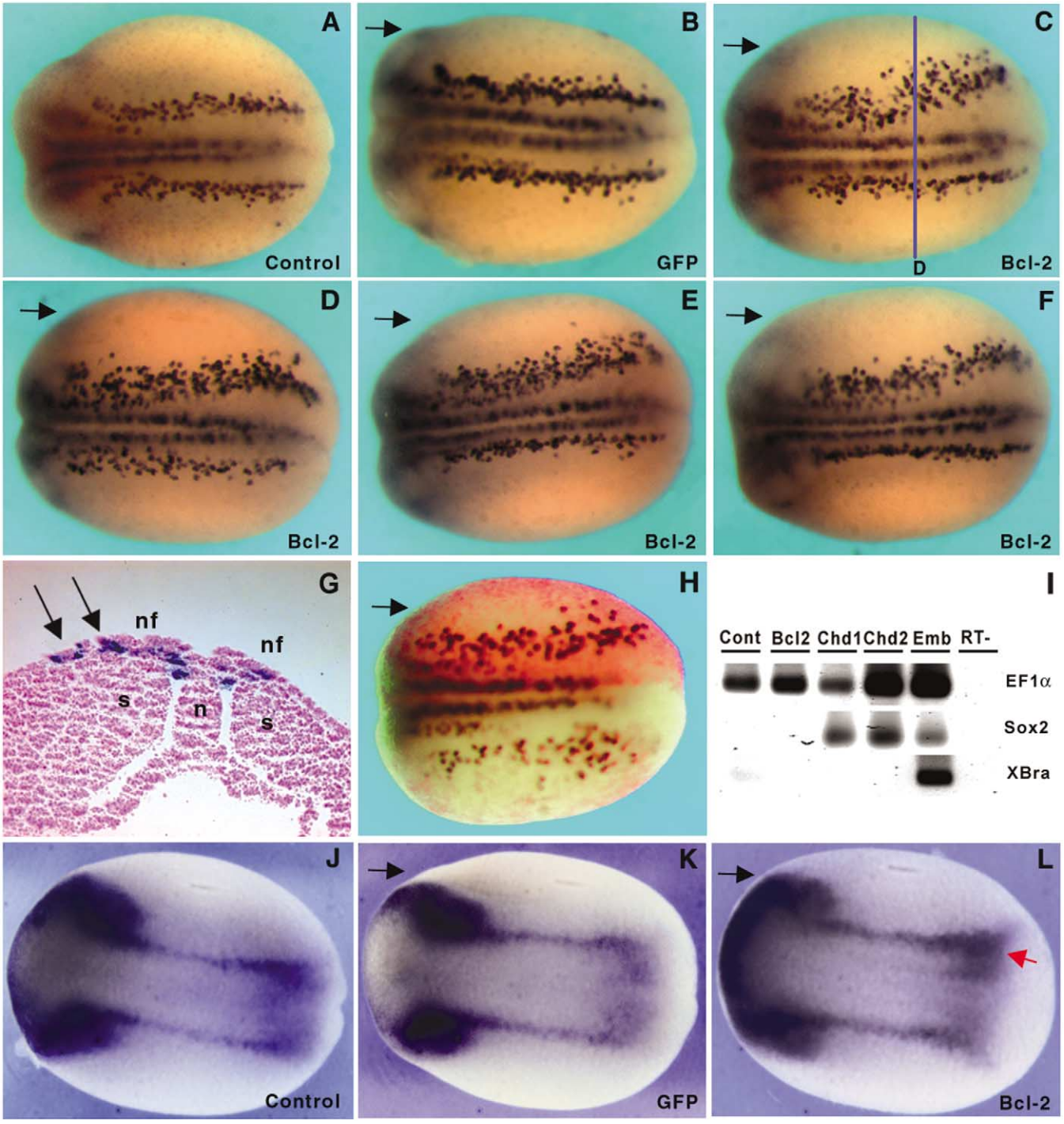

Fig. 3. Consequences of PCD Inhibition of PCD on primary neurogenesis. (A–F) Effect of PCD inhibition on *N-Tub* expression in stage 15 embryos as seen by whole-mount in situ hybridization; (A) uninjected control; (B) embryo injected unilaterally with *GFP* mRNA; (C–F) embryo injected unilaterally with *Bcl-2* mRNA. (C–F) Range of effect of PCD inhibition on domains of *N-Tub* expression. Injected embryos were injected at two-cell stage in one blastomere at 100–200 pg/nl. Arrows in (B-F) indicate the half that had been injected. (G) Transverse section taken from position indicated by the blue line from the embryo in (C). Arrows in (G) indicate the ectopic *N-Tub*-positive cells in the dorsal ectoderm; n, notochord; s, presomitogenic mesoderm; nf, neural fold. (H) Embryo injected unilaterally with *GFP* mRNA and subjected to immunocytochemistry with anti-GFP antibodies (red) and *in situ* hybridization with *N-Tub* probe (black). The injected half, stained in red, is indicated by an arrow. (I) RT-PCR analysis of stage 19 animal caps; Cont, uninjected control; Bcl-2, embryos injected with *Bcl-2* mRNA (100 pg/nl); Chd1, *Chordin* mRNA (20 pg/nl); Chd2, *Chordin* mRNA (100 pg/nl); Emb, whole embryo; RT−, RT-negative control. Primers specific for *EF-1α*, *XSox-2*, and *Xbra* were used. (J–L) Effect of PCD inhibition on *XZicr-2* expression in stage 15 embryos as seen by whole-mount in situ hybridization; (J) uninjected control; (K) embryo injected unilaterally with *GFP* mRNA; (L) embryo injected unilaterally with *Bcl-2* mRNA; red arrow indicates the posterior region which is expanded in the *Bcl-2*-injected half. Injected embryos were injected at two-cell stage in one blastomere at 100 pg/nl. Arrows indicate the injected halves. All embryos are shown in the dorsal orientation.

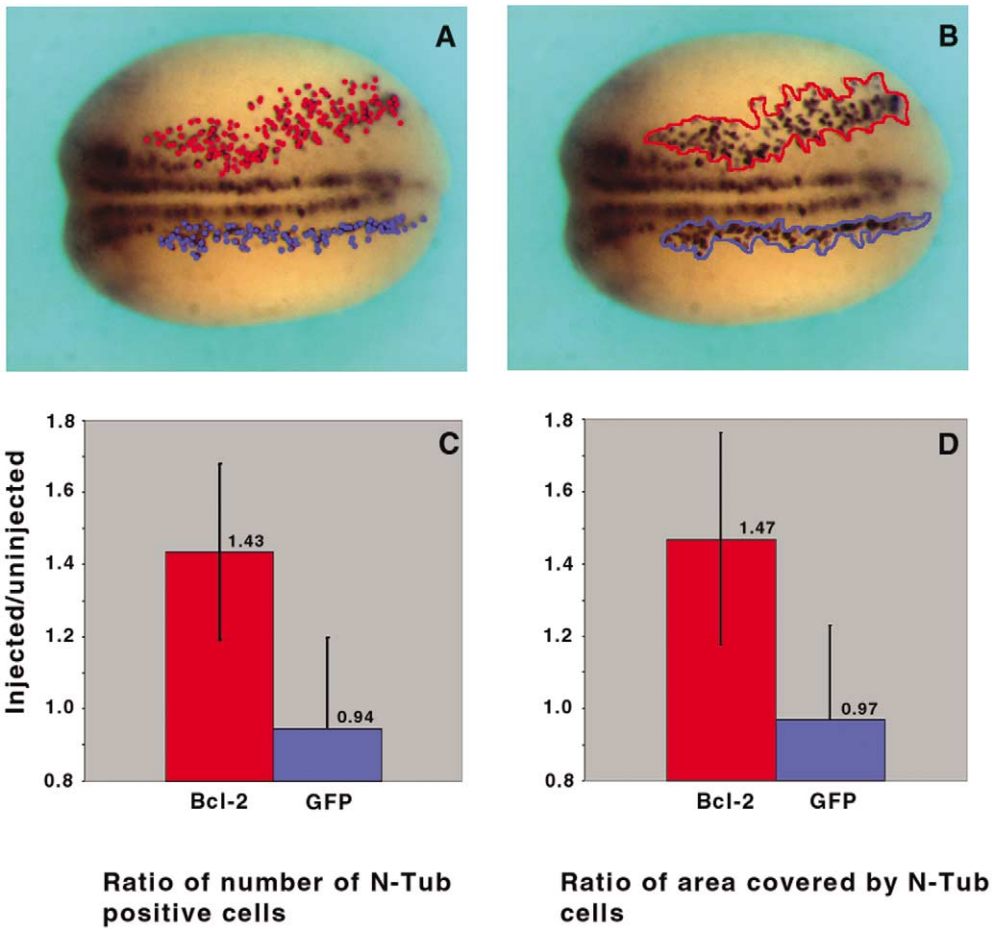

Fig. 4. Quantification of *N-Tubulin*-expressing cells and *N-Tubulin* domains. (A, C) Effect of PCD inhibition on number of *N-Tub*-positive cells. (C) Average ratios of cell counts from the injected sides (red dots in (A)) to that of the uninjected sides (blue dots in (A)) were calculated for *Bcl-2*-injected batch (red bar) and *GFP*-injected batch (blue bar; see Materials and Methods). (B, D) Effect of PCD inhibition on the area covered by *N-Tub* positive cells. (D) Average ratios of area measurements from the injected sides (outlines in red in (B)) to that of the uninjected uninjected sides (outlined in blue in (B)) were calculated for *Bcl-2*-injected batch (red bar) and *GFP*-injected batch (blue bar; see Materials and methods).

(Fig. 5). Inhibition of PCD resulted in the expansion of the lateral domain of *XMyT-1* expression corresponding to the position of sensory neurons (Fig. 5C; 30.4% in 204 *Bcl-2*-injected embryos). This effect is highly similar to that observed for *N-Tub* following PCD inhibition, in that at the stage examined, only the lateral domain exhibited significant expansion. Expression of *XNgnr-1*, which lies upstream of *XMyT-1*, was also affected by the inhibition of PCD (Fig. 5F). In addition, *XNgnr-1* exhibited a more significant phenotype following PCD inhibition, compared to its downstream genes, in that all three prospective neuronal domains were expanded at the stage examined (domains indicated by the red arrows in Fig. 5F). Further experiments revealed that the penetrance of embryos exhibiting expansion in *XNgnr-1* was higher than that of *N-Tub* (49.6% for *XNgnr-1* vs 30.5% for *N-Tub* in $\geq$300 embryos at 1.5 ng/embryo of *Bcl-2* mRNA; *t*-test value <0.05). Control embryos microinjected with *GFP* mRNA did not exhibit any significant changes in the expression of either gene when compared to the uninjected controls (Figs. 5B and E). These observations, together with the effect on *N-Tub* expression, indicate that the lack of PCD results in the expansion of gene expressions regulating neuronal differentiation, suggesting that PCD is likely to play a role during the differentiation of the posterior neuroecotoderm.

We wanted to determine if all neural tissues would be affected by the inhibition of PCD, in particular the anterior neural tissue, as PCD is at times localized within the anterior regions (Hensey and Gautier, 1998). We monitored *XSox-2* expression, which occurs shortly after neural induction, in a pan-neural manner (Mizuseki et al., 1998). Expression of *XSox-2* in the posterior neuroectoderm was expanded in the *Bcl-2*-injected side of the embryo, compared to that of the uninjected side, in agreement with the expansion of the domains of genes involved with differentiation of the posterior neuroectoderm (Fig. 5I; 38.0% in 84 *Bcl-2*-injected embryos). There was no significant difference between the pattern of *XSox-2* expression in the injected and uninjected sides of *GFP*-injected embryos, compared to that of the uninjected controls (Figs. 5H and K).

Furthermore, *XSox-2* expression in the anterior neuroectoderm was also expanded (Fig. 5L). This indicates that PCD is required for the development of the anterior neuroectoderm, as well as for the posterior neuroecoterm.

To investigate whether inhibition of PCD affected mesoderm tissues in addition to the neuroectoderm, we followed the expression of *XMyoD. XMyoD* is a bHLH transcription factor, expressed in the paraxial mesoderm, involved in the somitogenic differentiation of the paraxial mesoderm (Fig. 5M, Hopwood et al., 1989). Consistent with our previous observation that PCD does not take place at detectable levels within the paraxial presomitogenic mesoderm (Hensey and Gautier, 1998), the expression of *XMyoD* in the presomitogenic mesoderm in the *Bcl-2*-injected side did not exhibit any difference from that of the uninjected side (Fig. 5O).

PCD and neuronal differentiation

We decided to further investigate the regulation of PCD occurring during the differentiation of the posterior neuroectoderm. Differentiation of *XNgnr-1*-expressing cells is regulated by lateral inhibition, via the interaction between *X-Notch-1* and *X-Delta-1* (Bellefroid et al., 1996; Ma et al., 1996). We first determined if the outcome of lateral inhibition would be affected by PCD inhibition as PCD could be an alternative to neuronal cell fate for a subpopulation of cells undergoing lateral inhibition. Indeed, the pattern of TUNEL (Figs. 6A and B) overlaps with that of *X-Delta-1* (Fig. 6C) and *XNgnr-1* (Fig. 6D) in midneurulae (stage 14). Any effect on the outcome of lateral inhibition results in changes of the density of *N-Tub*-positive cells within the three neuronal domains (Chitnis et al., 1995). Density of *N-Tub*-positive cells in embryos exhibiting expanded *N-Tub* expression following PCD inhibition was derived from the cell count and area measurement quantifications (Fig. 4). Data obtained showed that there was no change in the density of *N-Tub*-positive cells in embryos with increased neuronal cell counts (number/area for Bcl-2-injected embryos = 0.97), compared to that obtained for GFP-injected control embryos (number/area for GFP-injected embryos = 0.97). This indicates that PCD inhibition does not affect the outcome of lateral inhibition. In addition, this suggests that lateral inhibition still restricts the number of cells specified to express *N-Tub* within the expanded neuronal domains following PCD inhibition. Overexpression of dominant negative *X-Delta-1*^{STU} interferes with the activity of the endogenous *X-Delta-1* and biases the outcome of lateral inhibition, resulting in an increase in the number of differentiating neurons within the neuronal domains (Fig. 6H; Chitnis et al., 1995). However, there did not appear to be any appreciable increase in TUNEL staining in the half microinjected with *X-Delta-1*^{STU} mRNA (Figs. 6F and G; 139 embryos). As *X-Delta*^{STU} interferes with the outcome of lateral inhibition, this strengthens the idea that PCD does not take place downstream of lateral inhibition.

We wished to determine if PCD is associated with differentiation of the neuroectoderm. The overexpression of constitutively active *X-Notch*^{ICD} prevented differentiation in the neuroecotoderm, leading to an expansion of uncommitted neural cells, seen as in the increase in *XSox-2* (Fig. 6K) and reduction in *N-Tub* expressions (Fig. 6L, Coffman et al., 1993). This was performed in the absence of cell proliferation via HUA treatment to enhance TUNEL staining without affecting the neurogenic effect of either *X-Notch*^{ICD} or *X-Delta*^{STU} overexpression (Figs. 6E–L; Coffman et al., 1993). In embryos microinjected unilaterally with *X-Notch*^{ICD}, the injected half exhibited a significant reduction in TUNEL staining, compared to the uninjected half (Figs. 6I and J; 51% of 93 embryos). TUNEL was excluded from the cells overexpressing *X-Notch*^{ICD} within regions stained in green (GFP tracer; Figs. 6I and J). Reduction of cell death in the half overexpressing *X-Notch*^{ICD} suggests that PCD is associated with differentiation of the neural cells. Therefore, PCD is reduced when the neural cells are prevented from differentiating, linking the occurrence of PCD to neuronal differentiation.

Discussion

Early neural cell death

The PCD we have analyzed takes place within a mixed population of actively proliferating neural precursors and new postmitotic neuroblasts (de la Rosa and de Pablo, 2000). Importantly, occurrence of PCD during this early stage sets it apart from cell death occurring in terminally differentiated neurons as a result of lack of neurotrophic support for their survival (Raff et al., 1993). At the stages analyzed (14–16), PCD affects neural precursors and young neuroblasts have not yet acquired the connective properties characteristic of differentiated neurons and are not dependent on neurotrophic factors for survival. This is reminiscent of PCD occurring in the proliferative and newly postmitotic regions of the neuroproliferative regions in the CNS of mouse embryos (Blaschke et al., 1996, 1998). We have demonstrated that disruption of early neural PCD results in abnormal neurogenesis, indicating that it is a prerequisite for early neural development.

The major consequence of cell death inhibition is the presence of supernumerary cells or “rescued cells,” which are cells that were meant to die but were prevented from doing so. Overexpression of Bcl-2 in neurons of transgenic mice results in the occurrence of supernumerary neurons (Martinou et al., 1994). Similarly, we demonstrated that PCD inhibition through overexpression of Bcl-2, in *Xenopus* early neural development, results in increased number of both neural and neuronal cell types. Consequences of PCD inhibition could be either cell-autonomous, non-cell-autonomous or both. A cell-autonomous effect of PCD inhibition would lead to rescued cells adopting alternative cell fates and resulting in increased domains of gene ex-

pression within the neuroectoderm. A non-cell-autonomous effect could arise if the rescued cells influence neighboring cells to adopt alternative cell fates (Ruiz i Altaba, 1994). Since we are not able to monitor the fate of rescued cells from the point when they are prevented from dying, we cannot distinguish between these possibilities which are not mutually exclusive. Nevertheless, either possibility predicts that the rescued cells are able to perform biological functions, rather than to remain nonfunctional.

PCD in the neurogenic cascade

The spatio-temporal pattern of PCD during primary neurogenesis overlaps with the patterns of expression of several of the genes regulating early neural development (Hensey and Gautier, 1998). Indeed, both *X-Delta-1* and *XNgnr-1* expressions display a significant degree of overlap with TUNEL during primary neurogenesis. However, neither *X-Delta-1* nor *XNgnr-1* patterns are completely superimposable with that of TUNEL. DNA fragmentation of apoptotic cells detected by TUNEL is very transient and TUNEL detection is possible only within a small window of time during apoptosis. The effect of PCD inhibition on the expression of these genes may suggest the position(s) in the neurogenic cascade at which PCD takes place, which is important in unraveling the role PCD plays during neurogenesis. There is an increase in the amount of cells determined to become neurons following PCD inhibition, indicated by the increase in *XNgnr-1* expression domains (Chitnis et al., 1995; Ma et al., 1996). Expression of neuronal genes downstream of *XNgnr-1*, such as *XMyT-1* and *N-Tub*, is increased as well. Increase in the expression of these downstream genes could be solely due to the increase in *XNgnr-1* cells, implying that PCD inhibition probably occurs upstream of or at the same level of *XNgnr-1* expression along the neurogenic cascade. The effect of PCD inhibition on *XNgnr-1*, which is more significant than that on either *XMyT-1* or *N-Tub*, supports this hypothesis. More significantly, *XNgnr-1* activates lateral inhibition, which regulates the density of neurons with the *XNgnr-1* domains, by inducing *X-Delta-1* (Chitnis et al., 1995; Ma et al., 1996). If PCD is a fate regulated by lateral inhibition or if PCD occurs downstream of lateral inhibition, the densities of *XMyT-1* and *N-Tub* should be increased. We have shown that the density of *N-Tub*-positive cells within the neuronal domains is not affected by PCD inhibition. This indicates that PCD does not take place in cells which have undergone selection by lateral inhibition. Taken together, our data strongly suggest that ectopic neurons arise as a consequence of increased *XNgnr-1*-positive cells, implying that PCD occurring before or upon the onset of differentiation has been inhibited, thus positioning PCD upstream of, or at the same level as, *XNgnr-1* expression. One implication is that PCD is associated with the process of neuronal determination, which is regulated by *XNgnr-1*. The expression of *XNgnr-1* persists throughout the neurulation stages, suggesting continuation of neuronal determination beyond the initial appearance of *N-Tub*, and this could account for the continued occurrence of PCD during the neurulation stages.

PCD and neuronal determination

An attractive hypothesis is that PCD is a novel form of regulation during the transition of neural cells that are undetermined and undifferentiated to cells which have been determined to differentiate into neurons. Constitutive Notch signaling results in the reduction of neuronal determination, by maintaining the neural cells in an uncommitted nature, as seen by the reduction in *XNgnr-1* and increase in *XSox-2* expressions (Coffman et al., 1993; Ma et al., 1996). Overexpression of *X-Notch*^{ICD} also results in the reduction of PCD occurring within the neuroectoderm (Figs. 6I and J). Therefore, by preventing the cells from differentiating via constitutive Notch signaling, PCD is no longer taking place. This supports the idea that effects of PCD inhibition discussed earlier might be the consequence of PCD inhibition occurring at the level of *XNgnr-1* expression, which determines the neuroecotoderm for differentiation. However, increase in neuronal density mediated by dominant negative *X-Delta-1*^{STU} does not alter the pattern of PCD. The effect of *X-Delta-1*^{STU} may be too subtle to be detected, compared to that of *X-Notch*^{ICD}. As TUNEL displays a significant level of variability (Hensey and Gautier, 1998), slight changes to the level of TUNEL may go undetected. Since *X-Delta*^{STU} interferes with the outcome of lateral inhibition, this is in agreement with the conclusion that the majority of PCD observed during primary neurogenesis is independent of events taking place downstream of lateral inhibition. Inhibition of PCD also leads to the expansion of undifferentiated neural cells, expressing *XSox-2*, with the potential to become *XNgnr-1*-expressing neurons. It will be interesting to assess the effect of modulating *XNgnr-1* expression on PCD, since we cannot rule out that the decrease in PCD following *X-Notch*^{ICD} overexpression may be due to its ability to inhibit apoptosis, as suggested by observations made in hematopoietic cells overexpressing *X-Notch*^{ICD} (Miele and Osborne, 1999).

PCD and proliferation in the neuroectoderm

The spatio-temporal pattern of division is similar to that of PCD, suggesting a possible connection between these two physiological processes (Hartenstein, 1989; Saka and Smith, 2001). The balance between cell death and cell division is essential to maintain cell number within a tissue and PCD could participate in regulating cell number within the neuroectoderm (Conlon and Raff, 1999; Evan et al., 1995). However, we do not believe that the primary role of PCD is to maintain absolute cell numbers in the developing neuroectoderm. Neural plates in which one cell cycle has been prevented, containing half the normal number of cells as a result, still undergo “patterned” PCD. Therefore, the

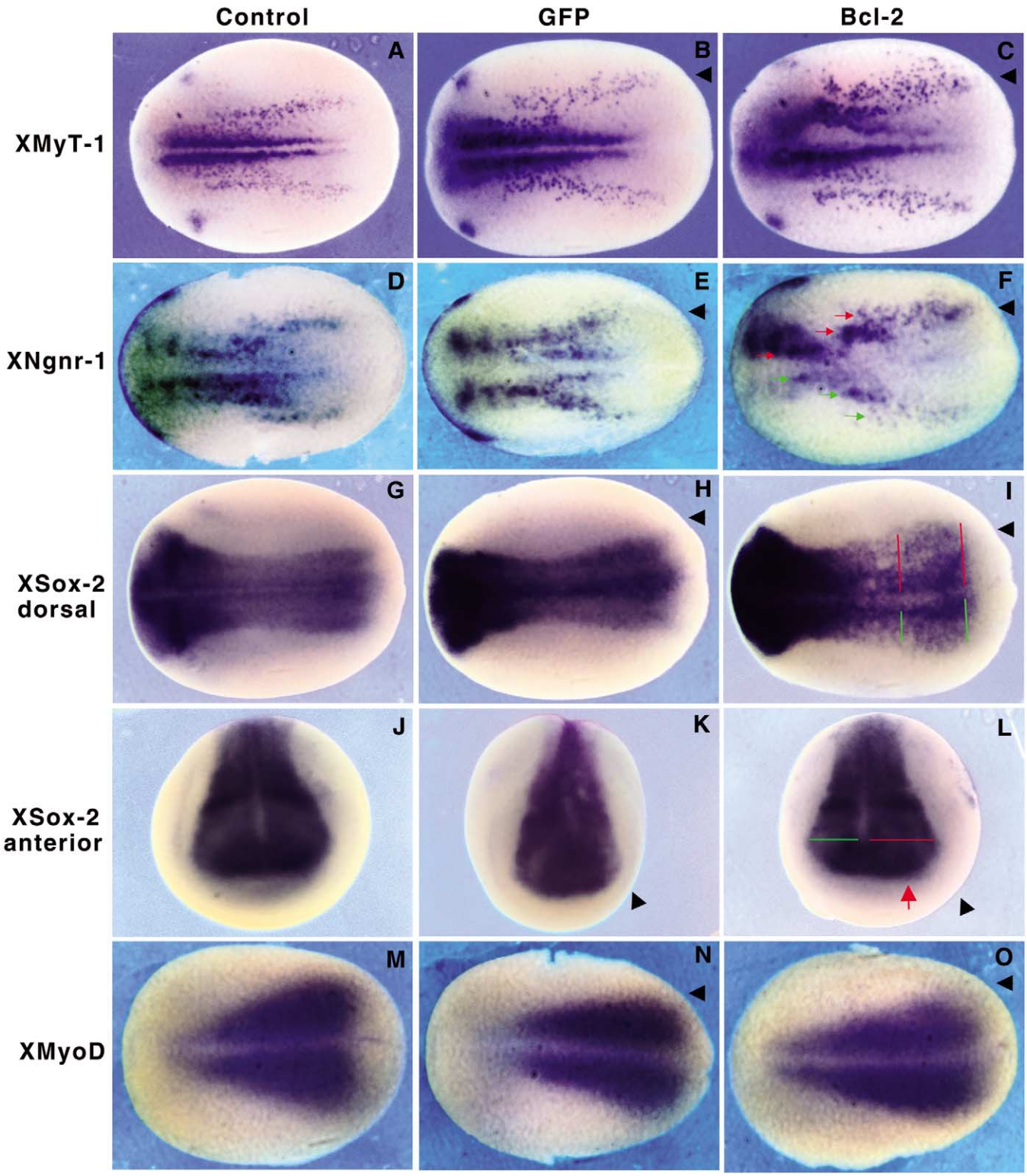

Fig. 5. Consequences of PCD inhibition on the expression of genes involved in primary neurogenesis. Effect of PCD inhibition on various neural markers is shown by whole-mount in situ hybridization. All injections were carried out on two-cell stage embryos in one blastomere; arrowheads in panels with injected embryos indicate the injected half. All embryos are shown in the dorsal orientation except for those in (M–O), which are shown in anterior orientation. (A, D, G, J, M) Uninjected control embryos; (B, E, H, K, N) embryos injected with *GFP* mRNA (100 ng/nl); (C, F, I, L, O) embryos injected with *Bcl-2* mRNA (100 ng/nl). Embryos were processed for in situ hybridization at stages 14–15 using probes specific for (A–C) *XMyT-1*, (D–F) *XNgnr-1;* red arrows in (F) indicate the three domains of neuronal differentiation in the Bcl-2-injected half and green arrows indicate the domains in the uninjected half, (G–L) *XSox-2;* red and green lines illustrate the expansion of *XSox-2* expression in the Bcl-2-injected half in (G) and (L); the red arrow in (L) indicates the expanded anterior neuroecotoderm in the injected half; (M–O) *XMyoD.*

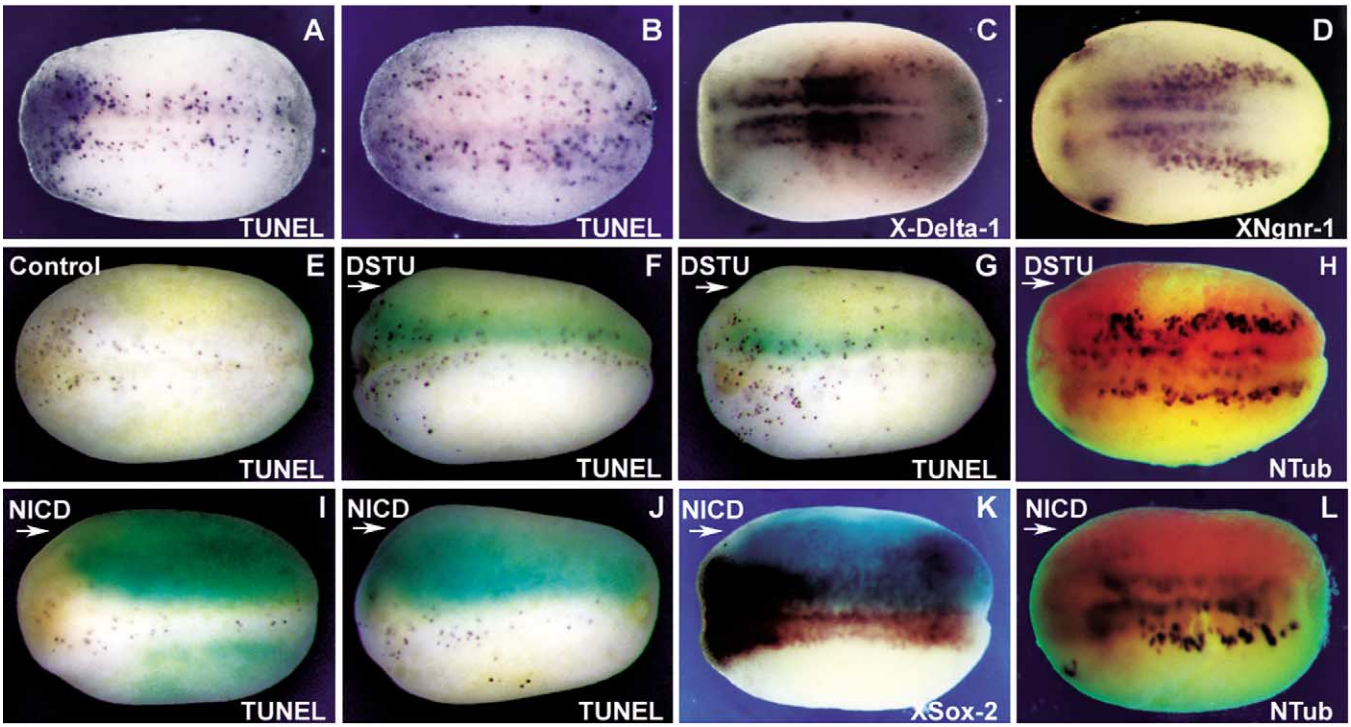

Fig. 6. Effect of overexpression of *X-Notch*^{ICD} on PCD. (A–D) Comparison between PCD pattern and *X-Delta-1* and *XNgnr-1* expression patterns in stage 15 midneurulae; (A, B) whole-mount TUNEL staining; (C, D) whole-mount *in situ* hybridization with probes specific for (C) *X-Delta-1* and (D) *XNgnr-1*. (E–L) Effect of overexpression of *X-Delta-1*^{STU} and *X-Notch*^{ICD} on neural development and PCD in embryos incubated with HUA; (E) uninjected control; (F–H) embryos coinjected unilaterally with *X-Delta-1*^{STU} and *GFP* mRNA (50 pg/nl); (I–L) embryos coinjected unilaterally with *X-Notch*^{ICD} mRNA (50 pg/nl) and GFP mRNA (50 pg/nl). Injected halves were visualized with immunocytochemistry with anti-*GFP* antibodies: green in (F, G, I, J); blue in (K); red in (H, L). Arrows in (F–H) and (I–L) indicate the injected halves. The embryos were also subjected to TUNEL (black) in (E, F, G, I, J) or in situ hybridization with probes specific for *N-Tubulin* (black) in (H, L), or *XSox-2* (brown) in (K). All embryos are in the dorsal orientation.

deficit in cell numbers of these HUA-treated embryos is not compensated by reduction in apoptosis.

It has also been proposed that cell death fate might require a certain number of divisions in some systems. However, PCD still occurs when the single round of cell division within the neuroectoderm between stages 12 and 16 is blocked. This demonstrates that the number of cell divisions does not determine the occurrence of PCD within the neuroectoderm. Interestingly, cell fate determination during primary neurogenesis is independent of cell division as well, confirming the more intimate interaction cell death has with the process of differentiation than it has with proliferation (Harris and Hartenstein, 1991).

Whereas the spatio-temporal pattern of PCD remains similar to that observed in control embryos, the amount of TUNEL staining is increased in HUA-treated embryos. The reasons for such an increase are not well understood. Part of the increased staining could possibly be a consequence of HUA treatment, following the block of cell cycle progression in S-phase. The ends of DNA replication intermediates, arising from incomplete replication, can potentially be labeled by TUNEL. However, inhibition of proliferation by HUA is not restricted to the neuroectoderm; cell division in other proliferating tissues, such as the lateral and ventral ectoderm, of the embryos is blocked as well, as seen in the overall reduction in immunocytochemistry staining with antibodies directed against phosphorylated histone H3 (Saka and Smith, 2001). Since there is no TUNEL staining observed within tissues other than the neuroectoderm, we can rule out the possibility that the increase in TUNEL staining is due to the labeling of blocked replicative structures. Furthermore, embryos treated with nocodazole, which blocks cell cycle progression in M-phase by interfering with the mitotic spindle (Hoebeke et al., 1976), also display increased TUNEL staining. Nocodazole-treated embryos still display a spatio-temporal TUNEL pattern similar to that in control embryos (data not shown).

Alternatively, blocking cell cycle progression could increase the sensitivity of TUNEL staining, possibly by lengthening the window of time during which apoptotic cells can be detected by TUNEL. Under normal conditions, TUNEL staining is absent in a fraction of embryos during gastrulation and neurulation (Hensey and Gautier, 1998). This may be due to the rapid degradation of apoptotic cells with a clearance time of 1 h or less (Jacobson et al., 1997). It is conceivable that cell cycle inhibition slows down the rate at which dying cells are degraded, thus allowing more cells to be detected by TUNEL at a given time. It has to be stressed that while HUA treatment enables better detection

of apoptotic cells, we do not believe that it increases the occurrence of PCD within the neuroectoderm.

In summary, we have shown that the inhibition of PCD is possible through the overexpression of anti-apoptotic Bcl-2 during early *Xenopus* embryogenesis. Using this system, we show that PCD is required for normal neural development in the early stages of embryogenesis; inhibition of PCD disrupts normal primary neurogenesis. This establishes that some neural cells undergo PCD as part of the normal neural development. *XNgnr-1* domains are most significantly affected by PCD inhibition, indicating that PCD is most prominent at the level of neuronal determination, leading to an increase of determined cells which will be subsequently selected for neuronal differentiation by lateral inhibition. While PCD is not involved in the maintenance of absolute cell number in the neuroectoderm, it is dependent on the amount of neuronal determination. By maintaining the neural cells uncommitted, PCD is abrogated, supporting the idea that PCD is associated with events that determine neural cells to become neurons.

Acknowledgments

We thank Jessica Greenwood, David Shechter, Dr. B. Feierbach, and Dr. K. Joubin for helpful discussion and comments on the manuscript. We thank Dr. A. Srinivasan (Idun Pharmaceuticals, Inc.) for the CM1 antibody. We thank Drs. A. Carrasco, A. Hemmati-Brivanlou, C. Kintner, S. Korsmeyer, A. Ruiz I Altaba, Y. Sasai, T. Sato, and J. Smith for cDNA constructs.

References

Agius, E., Oelgeschlager, M., Wessely, O., Kemp, C., De Robertis, E.M., 2000. Endodermal nodal-related signals and mesoderm induction in Xenopus. Development 127, 1173–1183.

Bellefroid, E.J., Bourguignon, C., Hollemann, T., Ma, Q., Anderson, D.J., Kintner, C., Pieler, T., 1996. X-MyT1, a Xenopus C2HC-type zinc finger protein with a regulatory function in neuronal differentiation. Cell 87, 1191–1202.

Blaschke, A.J., Staley, K., Chun, J., 1996. Widespread programmed cell death in proliferative and postmitotic regions of the fetal cerebral cortex. Development 122, 1165–1174.

Blaschke, A.J., Weiner, J.A., Chun, J., 1998. Programmed cell death is a universal feature of embryonic and postnatal neuroproliferative regions throughout the central nervous system. J. Comp. Neurol. 396, 39–50.

Brewster, R., Lee, J., Ruiz i Altaba, A., 1998. Gli/Zic factors pattern the neural plate by defining domains of cell differentiation. Nature 393, 579–583.

Cecconi, F., Alvarez-Bolado, G., Meyer, B.I., Roth, K.A., Gruss, P., 1998. Apaf1 (CED-4 homolog) regulates programmed cell death in mammalian development. Cell 94, 727–737.

Chao, D.T., Korsmeyer, S.J., 1998. BCL-2 family: regulators of cell death. Annu. Rev. Immunol. 16, 395–419.

Chitnis, A., Henrique, D., Lewis, J., Ish-Horowicz, D., Kintner, C., 1995. Primary neurogenesis in Xenopus embryos regulated by a homologue of the Drosophila neurogenic gene Delta. Nature 375, 761–766.

Chitnis, A.B., 1999. Control of neurogenesis—lessons from frogs, fish and flies. Curr. Opin. Neurobiol. 9, 18–25.

Coffman, C.R., Skoglund, P., Harris, W.A., Kintner, C.R., 1993. Expression of an extracellular deletion of Xotch diverts cell fate in Xenopus embryos. Cell 73, 659–671.

Cole, L.K., Ross, L.S., 2001. Apoptosis in the developing zebrafish embryo. Dev. Biol. 240, 123–142.

Conlon, I., Raff, M., 1999. Size control in animal development. Cell 96, 235–244.

de la Rosa, E. J., de Pablo, F., 2000. Cell death in early neural development: beyond the neurotrophic theory. Trends Neurosci. 23, 454–458.

Desagher, S., Martinou, J.C., 2000. Mitochondria as the central control point of apoptosis. Trends Cell Biol. 10, 369–377.

Evan, G.I., Brown, L., Whyte, M., Harrington, E., 1995. Apoptosis and the cell cycle. Curr. Opin. Cell Biol. 7, 825–834.

Gavrieli, Y., Sherman, Y., Ben-Sasson, S.A., 1992. Identification of programmed cell death in situ via specific labeling of nuclear DNA fragmentation. J. Cell Biol. 119, 493–501.

Glucksmann, A., 1965. Cell death in normal development. Arch. Biol. 76, 419–437.

Hakem, R., Hakem, A., Duncan, G.S., Henderson, J.T., Woo, M., Soengas, M.S., Elia, A., de la Pompa, J.L., Kagi, D., Khoo, W., Potter, J., Yoshida, R., Kaufman, S.A., Lowe, S.W., Penninger, J.M., Mak, T.W., 1998. Differential requirement for caspase 9 in apoptotic pathways in vivo. Cell 94, 339–352.

Harland, R. M. (1991). In situ hybridization: An improved wholemount method for *Xenopus* embryos. In "Methods in Cellular Biology" (B.K. Kay and H.B. Peng, Eds.) Vol. 36, pp. 685–695, Academic Press, San Diego.

Harland, R., 2000. Neural induction. Curr. Opin. Genet. Dev. 10, 357–362.

Harris, W.A., Hartenstein, V., 1991. Neuronal determination without cell division in Xenopus embryos. Neuron 6, 499–515.

Hartenstein, V., 1989. Early neurogenesis in Xenopus: the spatio-temporal pattern of proliferation and cell lineages in the embryonic spinal cord. Neuron 3, 399–411.

Hensey, C., Gautier, J., 1997. A developmental timer that regulates apoptosis at the onset of gastrulation. Mech. Dev. 69, 183–195.

Hensey, C., Gautier, J., 1998. Programmed cell death during Xenopus development: a spatio-temporal analysis. Dev. Biol. 203, 36–48.

Hirata, M., Hall, B.K., 2000. Temporospatial patterns of apoptosis in chick embryos during the morphogenetic period of development. Int. J. Dev. Biol. 44, 757–768.

Hoebeke, J., Van Nijen, G., De Brabander, M., 1976. Interaction of oncodazole (R 17934), a new antitumoral drug, with rat brain tubulin. Biochem. Biophys. Res. Commun. 69, 319–324.

Hopwood, N.D., Pluck, A., Gurdon, J.B., 1989. MyoD expression in the forming somites is an early response to mesoderm induction in Xenopus embryos. EMBO J. 8, 3409–3417.

Jacobson, M.D., Weil, M., Raff, M.C., 1997. Programmed cell death in animal development. Cell 88, 347–354.

Kerr, J.F., Wyllie, A.H., Currie, A.R., 1972. Apoptosis: a basic biological phenomenon with wide-ranging implications in tussue kinetics. Br. J. Cancer 26, 239–257.

Kuan, C.Y., Roth, K.A., Flavell, R.A., Rakic, P., 2000. Mechanisms of programmed cell death in the developing brain. Trends Neurosci. 23, 291–287.

Kuida, K., Haydar, T.F., Kuan, C.Y., Gu, Y., Taya, C., Karasuyama, H., Su, M.S., Rakic, P., Flavell, R.A., 1998. Reduced apoptosis and cytochrome c-mediated caspase activation in mice lacking caspase 9. Cell 94, 325–337.

Kuida, K., Zheng, T.S., Na, S., Kuan, C., Yang, D., Karasuyama, H., Rakic, P., Flavell, R.A., 1996. Decreased apoptosis in the brain and premature lethality in CPP32-deficient mice. Nature 384, 368–372.

Ma, Q., Kintner, C., Anderson, D.J., 1996. Identification of neurogenin, a vertebrate neuronal determination gene. Cell 87, 43–52.

Martinou, J.C., Dubois-Dauphin, M., Staple, J.K., Rodriguez, I., Frankowski, H., Missotten, M., Albertini, P., Talabot, D., Catsicas, S.,

Pietra, C., et al., 1994. Overexpression of BCL-2 in transgenic mice protects neurons from naturally occurring cell death and experimental ischemia. Neuron 13, 1017–1030.

Miele, L., Osborne, B., 1999. Arbiter of differentiation and death: notch signaling meets apoptosis. J. Cell Physiol. 181, 393–409.

Mizuseki, K., Kishi, M., Matsui, M., Nakanishi, S., Sasai, Y., 1998. Xenopus Zic-related-1 and Sox-2, two factors induced by chordin, have distinct activities in the initiation of neural induction. Development 125, 579–587.

Nicholson, D.W., Thornberry, N.A., 1997. Caspases: killer proteases. Trends Biochem. Sci. 22, 299–306.

Nieuwkoop, P.D., Faber, J., 1967. Normal Table of *Xenopus laevis*. Daudin, North-Holland, Amsterdam.

Oschwald, R., Richter, K., Grunz, H., 1991. Localization of a nervous system-specific class II beta-tubulin gene in *Xenopus laevis* embryos by whole-mount in situ hybridization. Int. J. Dev. Biol. 35, 399–405.

Raff, M.C., Barres, B.A., Burne, J.F., Coles, H.S., Ishizaki, Y., Jacobson, M.D., 1993. Programmed cell death and the control of cell survival: lessons from the nervous system. Science 262, 695–700.

Ruiz i Altaba, A., 1994. Pattern formation in the vertebrate neural plate. Trends Neurosci. 17, 233–243.

Saka, Y., Smith, J.C., 2001. Spatial and temporal patterns of cell division during early Xenopus embryogenesis. Dev. Biol. 229, 307–318.

Sanders, E.J., Wride, M.A., 1995. Programmed cell death in development. Int. Rev. Cytol. 163, 105–173.

Sasai, Y., 1998. Identifying the missing links: genes that connect neural induction and primary neurogenesis in vertebrate embryos. Neuron 21, 455–458.

Sive, H.L., Grainger, .M., Harland, R.M., 1994. Early Development of *Xenopus laevis*. Cold Spring Harbor Laboratory Press, Cold Spring Harbor, NY.

Srinivasan, A., Roth, K.A., Sayers, R.O., Shindler, K.S., Wong, A.M., Fritz, L.C., Tomaselli, K.J., 1998. In situ immunodetection of activated caspase-3 in apoptotic neurons in the developing nervous system. Cell Death Differ. 5, 1004–1016.

Talanian, R.V., Quinlan, C., Trautz, S., Hackett, M.C., Mankovich, J.A., Banach, D., Ghayur, T., Brady, K.D., Wong, W.W., 1997. Substrate specificities of caspase family proteases. J. Biol. Chem. 272, 9677–9682.

Yin, X.M., Oltvai, Z.N., Korsmeyer, S.J., 1994. BH1 and BH2 domains of Bcl-2 are required for inhibition of apoptosis and heterodimerization with Bax. Nature 369, 321–323.

Yoshida, H., Kong, Y.Y., Yoshida, R., Elia, A.J., Hakem, A., Hakem, R., Penninger, J. M., Mak, T.W., 1998. Apaf1 is required for mitochondrial pathways of apoptosis and brain development. Cell 94, 739–750.